LIST OF CONTRIBUTORS

E. Arzt
H. Biloni
J.L. Bocquet
G. Brébec
R.W. Cahn
G.Y. Chin
R.D. Doherty
H.E. Exner
G. Frommeyer
D.R. Gaskell
K. Girgis
H. Gleiter
P. Haasen
J.P. Hirth
E.D. Hondros
E. Hornbogen
W.L. Johnson
H.W. King
G. Kostorz
Y. Limoge
J.D. Livingston
F.E. Luborsky
T.B. Massalski
R.F. Mehl †
P. Neumann
A.D. Pelton
D.G. Pettifor
M. Rühle
M.P. Seah
J.-L. Strudel
R.M. Thomson
C.M. Wayman
J. Weertman
J.R. Weertman
M. Wilkens
H.J. Wollenberger

PHYSICAL METALLURGY

Third, revised and enlarged edition

Edited by

R.W. CAHN
Université de Paris-Sud, France

P. HAASEN
Universität Göttingen, Germany

PART II

1983

NORTH-HOLLAND PHYSICS PUBLISHING
AMSTERDAM – OXFORD – NEW YORK – TOKYO

CHAPTER 30

SINTERING PROCESSES

H.E. EXNER and E. ARZT

Max-Planck-Institut
Institut für Werkstoffwissenschaften
7000 Stuttgart 1, FRG

R.W. Cahn and P. Haasen, eds.
Physical Metallurgy; third, revised and enlarged edition
© Elsevier Science Publishers BV, 1983

Introduction

The technique of forming metal parts from powders by pressing and sintering dates back to the beginning of human civilization. Almost every metal or ceramic material was initially made via the powder route. Modern applications of sintering in materials technology are widespread: powder-metallurgical production of structural steel parts, self-lubricating bearings, porous metals for filtering, tungsten wires for lamp filaments, soft and hard magnetic materials, electrical contacts, cemented carbides for cutting tools and a large variety of ceramic components are only a few of the many technical production processes involving sintering as an important step. A recent book by LENEL [1980] gives a comprehensive review. Sintering processes are also important in a number of other fields of materials technology. One example is sintering of finely ground ores into pellets, thereby preparing them for smelting. On the other hand, sintering of finely dispersed catalyst materials at operating temperatures is undesirable since it lowers their activity.

The consolidation of powders and densification of porous solids is possible by pressing and subsequent pressureless heat-treatment (*solid-state sintering*), by simultaneous application of pressure and heat (*hot-pressing* or *pressure-sintering*) or with the aid of a limited amount of melt (*liquid-phase sintering*). The technology of sintering and hot-pressing has been thoroughly developed down to minute details. Physicists, chemists, metallurgists and ceramists have worked together to establish the theoretical basis for understanding the complex interaction of geometrical and thermodynamic factors and the effects of a number of mechanisms which occur simultaneously or in sequence. Some of these results are discussed in the following.

1. Solid-state sintering

In the majority of technical applications, powders are compacted into shaped parts which then are heat-treated in order to give them the required mechanical and physical properties. The essential difference between a powder (or a porous body) and a dense solid body of exactly the same material and identical mass is, from the energetic point of view, the excess free energy due to the broken atomic bonds at the surface. Stressing this fundamental aspect, we can define *pressureless sintering* as material transport driven by surface energy or, in other words, by capillary forces. This material transport involves several basic mechanisms, essentially of diffusional-flow type. By filling in the necks at the points of contact between the powder particles and, at a later stage, the pore space, sintering increases density and strength of the compacted powders.

Figure 1 shows neck formation between spherical copper particles, and fig. 2 shows the geometrical changes taking place during sintering of tungsten powder. There are numerous experimental methods for studying the progress of sintering in laboratory experiments, reviewed recently by EXNER [1980]. Table 1 gives a summary of the frequently used techniques. In the following we will focus on experimental

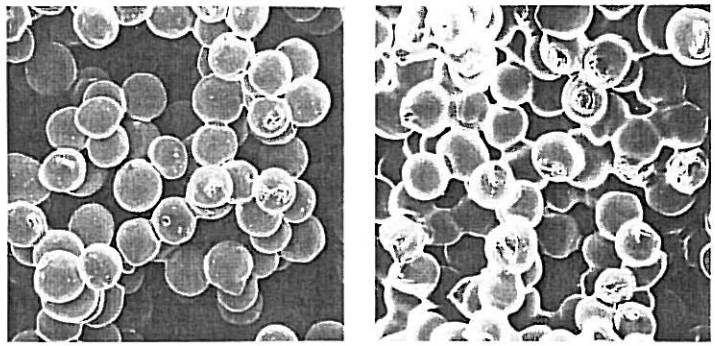

Fig. 1. Neck formation between loosely packed spherical copper particles during sintering at 1300 K for 1 h (left) and 8 h (right). 150×.

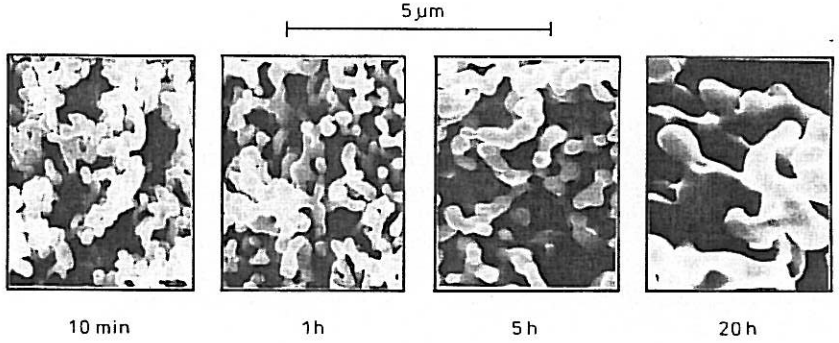

Fig. 2. Fine tungsten powder sintered in hydrogen at 1470 K for 10 min, 1 h, 5 h, and 20 h (from left to right). (After EXNER [1979a].)

facts elucidating the basic phenomena and on the theoretical concepts for quantifying sintering mechanisms.

1.1. Driving energy

Surface energy provides the motivation of material transport during pressureless sintering. Its magnitude can be estimated theoretically or determined experimentally in various ways and ranges for metals, alloys, intermetallic compounds and non-metallic crystalline solids from a tenth to a few J/m^2 (for references see ROTH [1975] and EXNER [1982]). The most reliable and instructive technique of visualizing the effect and measuring the value of surface energy is the so-called *zero-creep* technique

References: p. 1908.

Table 1
Experimental method for deriving quantitative information on changes of pore geometry during sintering.

Method	Quantity measured	Remarks
Dilatometry	Length change	Shrinkage may vary in different directions. Relative precision approximately 10^{-6} of sample length.
Buoyancy	Density	Impregnation or pore sealing necessary. Relative precision approximately 10^{-3}.
Gas	Solid–pore interface	Only for high specific interfaces (> 0.1 m^2/cm^3). Closed pores not included. Relative precision approximately 10^{-2} for total areas > 0.5 m^2.
Porosimetry	Accessible pore volume	For open and fine pore systems. Interpretation of pressure–volume diagrams difficult.
Indirect methods	Physical properties	Exact relationships between pore geometry and properties usually not known.
Quantitative microscopy	Direct geometric parameters	Tedious but most effective method for complete characterization of pore geometry.

first described by UDIN *et al.* [1949]. This technique is described in ch. 13, § 3.1.

Depending on the size of the powder particles or the amount and dispersion of porosity in a compact, the total excess energy of the surface amounts to 0.1–100 J per mole of solid where the smaller number applies to coarse powders (~ 100 μm diameter) and to low-porosity material and the larger number to submicron powders or highly dispersed porosity. Grain-boundary energy usually provides a back-driving force because, at least in the early stages, new grain boundaries are formed while the particle contacts are being filled in (fig. 3). For most materials (especially metals)

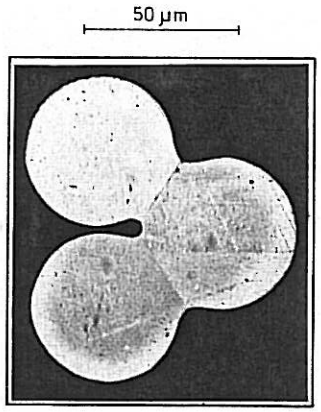

Fig. 3. Metallographic cross-section through an arrangement of three copper particles sintered at 1300 K for 8 h. Note the grain boundaries in the necks. (From EXNER [1979a].)

grain-boundary energies are lower (approximately by a factor of three) than surface energies, and the dihedral angle is of the order of 160°. Therefore the back-driving effect is not very pronounced. However, as pointed out by HOGE and PASK [1977], material transport during sintering may cease because of the establishment of local equilibrium between grain-boundary- and surface energy in cases where the grain-boundary energy is high (dihedral angle $< 120°$).

If a volume element dV is removed from ($dV < 0$) or added to ($dV > 0$) a surface with the principal radii of curvature r_1 and r_2, the energy change, dE, involved is

$$\frac{dE}{dV} = \gamma \frac{dA}{dV} = \gamma\left(\frac{1}{r_1} + \frac{1}{r_2}\right), \tag{1}$$

where γ is the (isotropic) surface energy and dA is the change in surface area. dE/dV formally corresponds to a stress, σ, which leads to the well-known Laplace equation

$$\sigma = \gamma\left(\frac{1}{r_1} + \frac{1}{r_2}\right). \tag{2}$$

Fig. 4. High-porosity beryllium alloy produced from cobalt-coated beryllium particles by sintering. 1000×. (From ALDINGER [1974].)

References: p. 1908.

Under a concave surface, this stress is tensile and under a convex surface, compressive. Therefore, a stress gradient exists between the particle interior and the neck. Similarly, a gradient in chemical potential can be defined which, in turn, corresponds to a gradient of vapour pressure (Kelvin equation) or vacancy concentration (Thomson–Freundlich equation, see ch. 6, § 9.3). Owing to the stress gradient, the difference in vapour pressure, or the gradient in vacancy concentration, material is transported by viscous flow (in amorphous materials), by plastic flow, evaporation/vapour transport/condensation, diffusion along the surface and grain boundaries, or volume diffusion.

Chemical driving forces due to nonequilibrium composition of powders (e.g. mixture of elemental powders which react at sintering temperature) are usually much higher than capillary forces. This fact, which becomes apparent by merely comparing the molar surface energies with energies of mixing or compound formation, has been demonstrated in models, e.g. by sintering a cobalt sphere to a nickel plate (THÜMMLER and THOMMA [1966]). The same effect causes the well-known Kirkendall porosity (ch. 5, § 5.3) and has been used to prepare highly porous bodies from nickel or cobalt-covered beryllium spheres, as shown in fig. 4. However, in special cases chemical driving forces can be overcome by capillary forces: owing to the higher diffusivity of indium, an intermetallic compound is formed at the neck region between two wires of an originally homogeneous solid solution of copper–indium (KUCZYNSKI *et al.* [1960]), and silver is enriched in the neck region between initially homogeneous Ag–Au spheres (MISHRA *et al.* [1975]). However, rehomogenization occurs as soon as the sharp curvatures at the neck surface are filled in and capillary forces are reduced. Chemical effects, which play a major role in most real systems, must clearly be differentiated from ideal surface-energy controlled sintering.

1.2. Material sinks and sources

Possible sinks and sources for material (or vice versa for vacancies) are the surface (pore–solid interface), grain boundaries, and dislocations. The role of the surface is clear: Since surface energy is reduced when concave regions are filled in, these regions (in the early stages predominantly the highly concave neck surface, in the later stages the concave parts of the pore–solid interface) are the sinks for material (or the sources of vacancies). The convex part of the particle surface or solid–pore interface is one of the material sources. It is obvious that redistribution of material over the surface by surface and/or volume diffusion will not result in shrinkage of the compact or reduction of pore space (i.e. densification) but can only increase strength by enlarging the contact areas and reducing the notch effect of sharp pore contours.

Densification occurs when material is removed from the volume between the particle contacts. In numerous experiments, the decisive role of grain boundaries as sinks for vacancies arriving from the neck surface or pores has been demonstrated (ALEXANDER and BALLUFFI [1957], ICHINOSE and KUCZYNSKI [1962]; for further references see GEGUZIN [1973], USKOKOVIĆ and EXNER [1977], and EXNER [1979a]).

Pores shrink only when attached to or located very close to grain boundaries, and particle centres approach each other only when the particles are separated by at least one grain-boundary. A most convincing experiment is the comparison of shrinkage rates of sintered copper with a high density of grain boundaries, resulting in pronounced shrinkage, with that of dezincified brass with a low density of grain boundaries, showing virtually no shrinkage (BRETT and SEIGLE [1963]).

Grain boundaries are usually assumed to be perfect vacancy sinks at the supersaturation levels caused by capillarity, but recent models for the structure of grain boundaries (ASHBY *et al.* [1978], BALLUFFI [1980], ch. 10B, § 2.2) assume a fairly well-defined structure that would be disrupted if atoms were removed. This leads to the suggestion (ASHBY [1972], ARZT *et al.* [1982]) that a divergence of the diffusive flux of matter can occur only at dislocation-like defects (grain-boundary dislocations as observed, for example, by GLEITER [1969], SCHOBER and BALLUFFI [1970], NILSSON *et al.* [1979] and KING and SMITH [1980]). The details of these dislocation structures (ch. 10B, § 2.2) can depend on the misorientation of the adjacent grains. By emitting atoms, these defects move in a non-conservative way in the boundary plane. The effectiveness of a grain boundary as a source for atoms or sink for vacancies is thus determined by the mobility of the grain-boundary dislocations, which may be reduced by solute atoms exerting a viscous drag, or by grain-boundary particles pinning the dislocations. The pronounced dependence of neck growth upon orientation between a zinc single crystal sphere and a zinc plate (NUNES *et al.* [1971]), the variation of neck sizes between simultaneously sintered copper spheres (EXNER [1979a]), the low apparent diffusivities observed in some sintering experiments (for references see EXNER [1979a]) or the complete suppression of shrinkage in metals containing dispersed particles (ASHBY *et al.* [1980]) can be understood in these terms, as well as the effect of grain-boundary structure in zero-creep experiments (JAEGER and GLEITER [1978]). (In this connection see also ch. 25, § 3.4.1.)

There is more or less general agreement that lattice dislocations cannot be generated under the action of capillary stresses prevailing during sintering. Nevertheless, high densities of lattice dislocations have been observed in regions close to the grain boundary of a particle sintered to a plate and it has been suggested that these dislocations may contribute to the shrinkage in various ways (SCHATT *et al.* [1982]). For example, diffusion can take place from one dislocation to another, which can result in removal of atomic planes in the direction of compressive stress and insertion of those under tension. Lattice dislocations then act both as vacancy sources and sinks, and move non-conservatively by climb (NABARRO [1967], SCHATT [1981]). Obviously, increased dislocation density in the neck region would also provide short-circuits for diffusion and thus reduce the effective diffusion distance between material sinks and sources.

1.3 Neck growth and shrinkage equations

There have been a large number of attempts to quantify the kinetics of neck growth and shrinkage. Early work dating back to the time between the two World

References: p. 1908.

Table 2
Constants appearing in eqs. (3) and (5) (after EXNER [1979a]).

Transport Mechanism	Range		Plausible Values [b]		
	n	m	n	m	C
Viscous flow	2	1	2	1	$\frac{3\gamma}{2\eta}$
Evaporation and recondensation [a]	3–7	2–4	3	2	$3\cdot\sqrt{\frac{2}{\pi}}\,\frac{r\gamma pM^{3/2}\rho^{1/2}}{(RT)^{3/2}}$
Grain-boundary diffusion	6	4	6	4	$\frac{48\gamma\cdot D_b\cdot b\cdot M}{RT}$
Volume-diffusion from the grain boundary	4–5	3	5	3	$\frac{16D_V\cdot\gamma\cdot M}{RT}$
Volume diffusion from the surface [a]	4	3	4	3	$\frac{20D_V\cdot\gamma\cdot M}{RT}$
Surface diffusion [a]	3–7	2–4	7	4	$\frac{23\gamma\cdot D_s\cdot w\cdot M}{RT}$

[a] No centre approach, $h/a \equiv 0$.
[b] With the symbols in the expressions for C denoting:

D_b, D_S, D_V = diffusion coefficients for grain boundary, surface and volume diffusion; M = molar volume; R = gas constant; T = absolute temperature; b = grain-boundary width; p = gas pressure; w = width of surface atom layer; γ = specific surface energy; η = viscosity constant; ν = accomodation coefficient for gas transport; ρ = specific gravity.

Wars (TAMMANN [1926], HEDVALL and HELIN [1927] and BALSHIN [1936]) is characterized by intuition rather than by physical reasoning (GEGUZIN [1973]). Some of the important fundamental ideas can be found in papers published around 1950 (e.g. FRENKEL [1945], JONES [1946], PINES [1946], HÜTTIG [1948], SHALER and WULFF [1948], MACKENZIE and SHUTTLEWORTH [1949] and CLARK and WHITE [1950]). In particular, the work by KUCZYNSKI [1949] and HERRING [1950] marks the beginning

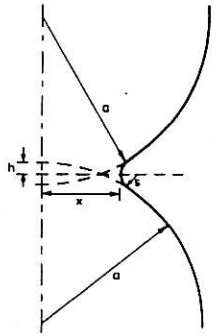

Fig. 5. Geometry of an idealized neck contour between two spherical particles (a = particle radius, x = neck radius, s = radius of neck curvature for a tangent circle, h = half of the centre approach and particle interpenetration).

of a quantitative modelling of sintering processes. Several research schools have developed since then in the various parts of the world (for reviews see FISCHMEISTER and EXNER [1964], THÜMMLER and THOMMA [1967], GEGUZIN [1973] and EXNER [1979a]). The classical approach has been the study of two coalescing particles (Frenkel–Kuczynski model), usually spheres or rods, in order to reduce problems inherent in the highly complicated geometry of powder compacts. Using idealized neck shapes (cylindrical or toroidal necks which result in contours formed by tangent circles, see fig. 5), analytical relationships were derived for the time- and particle-size dependence of neck size, x, during isothermal sintering. These equations are generally of power-law type

$$(x/a)^n = Ca^{-m}t \tag{3}$$

where a is the radius of the spherical or cylindrical particles in contact which each other, t is the time of isothermal sintering, and n, m and C are constants which are typical for the individual transport mechanism. Table 2 (see also COBLENZ *et al.* [1980], and GERMAN [1982]) lists the range of values of n and m given in the literature and plausible values for n, m and C following derivations by FRENKEL [1945] for viscous flow, by KINGERY and BERG [1955] for evaporation and condensation, and by ROCKLAND [1967] for the diffusional transport mechanisms. From the neck growth the amount of interpenetration of the two particles, and thus the centre approach between the two particles, can be estimated. Evaporation and condensation, volume diffusion from the surface, and surface diffusion cannot produce centre approach. For the other mechanisms it is assumed that all the material filling the neck comes from the grain boundaries in contact regions, and using again the idealized geometry and neglecting second-order terms, the approach of the two particle centres, $2h$, (see fig. 5) can be estimated from the neck size, x:

$$h = x^2/4a. \tag{4}$$

Using eq. (3), the time- and temperature dependence of the relative centre approach, h/a, is:

$$(h/a)^{n/2} = 2^{-n}Ca^{-m}t, \tag{5}$$

with C, n and m shown in table 2 for the relevant mechanisms.

Viscous flow and volume diffusion can act on their own to remove material from regions between the particle centres while grain-boundary diffusion obviously needs the cooperation of another process to distribute the material reaching the surface at its intersection with the grain boundary, e.g. surface- or volume diffusion, which may then be rate-controlling (COBLE [1958], GESSINGER [1970], JOHNSON [1970] and SWINKELS and ASHBY [1980]). The major role of surface diffusion is to reshape the surface in such a way that the curvature gradient (and thus the chemical potential gradient) changes continuously over the surface and sharp curvatures are reduced quickly. This effect, termed *undercutting* (NICHOLS and MULLINS [1965]), is clearly revealed in fig. 6; it is particularly pronounced at the early stages of contact formation, producing a bulb-shaped neck contour.

References: p. 1908.

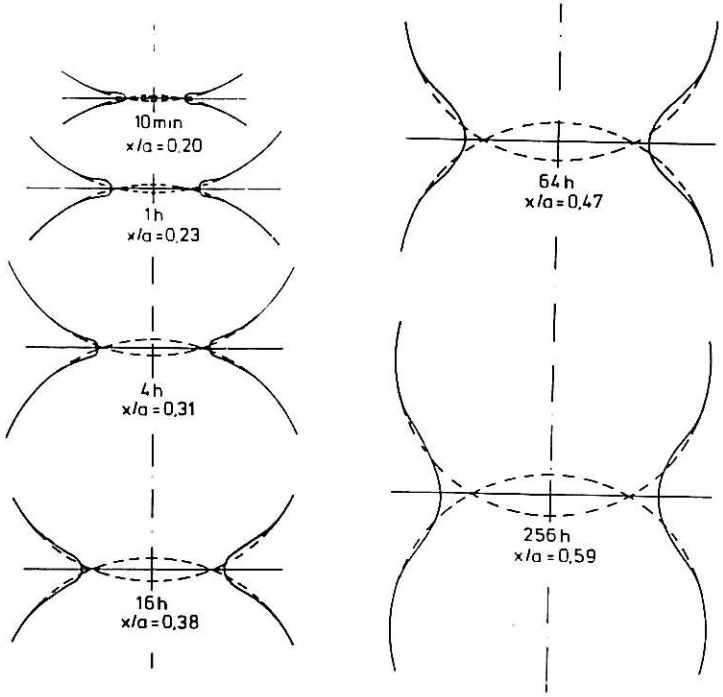

Fig. 6. Neck shapes developed between two copper spheres during sintering at 1200 K. The redistribution of material along the surface close to the neck causes undercutting. The dashed lines show the circular contours of the original particles, the fully drawn lines are taken from shadow-graphs. (From EXNER [1979a].)

There have been numerous attempts to derive equations for neck growth and centre approach for more realistic neck geometries and for simultaneously acting sintering mechanisms. Reviews and detailed discussions have been published recently by COBLENZ *et al.* [1979] and EXNER [1979a]. Analytical solutions are still possible for neck geometries with elliptical or cartenoid-shaped contours (SWINKELS and ASHBY [1980] and GERMAN and MUNIR [1975]), but numerical techniques must be applied for assumption-free modelling of neck shapes (for recent solutions and references see BROSS and EXNER [1979], EXNER [1979a], NICHOLS [1980] and ROSS *et al.* [1982]). Figure 7 shows, as an example, the geometry for simultaneous grain-boundary and surface transport obtained by computer simulation, which, compared to the simple tangent circle approximation, conforms much more closely to the experimental geometry (compare fig. 6).

The results of these complex calculations are not as easily visualized or applied as

the simple power laws [eqs. (3) and (5)] and, therefore, have not gained much popularity. Usually, however, application of the simple equations is taken too far in interpreting experimental work quantitatively, considering the severe geometric simplifications and the problems connected with superimposed mechanisms (in addition to chemical effects due to impurities, among other divergences between theoretical assumptions and real systems). The same restrictions must apply to *sintering maps* delineating the temperature and neck-size regions in which a specific material transport mechanism is predominant (ASHBY [1974] and SWINKELS and ASHBY [1981]). Unlike the *hot-pressing maps* discussed below (see figs. 12 and 13), these sintering-mechanism diagrams are rather limited for quantifying the effects of various sintering parameters for practical purposes owing to the severe simplifications they are based on. Nevertheless, they provide a convenient means of visualizing the results of theoretical calculations.

In spite of these principal deficiencies, the theoretical treatments and experiments based upon the two-particle approach have been highly successful in categorizing the active material-transport processes. There is general agreement that sintering of most metals and ceramics can be understood on the basis of *diffusional or Herring–Nabarro–Coble creep* (ch. 20, § 1.11) with surface diffusion playing a major role, while vapour transport and plastic flow play a minor part which, however, cannot be neglected in all cases. Most of the basic phenomena occurring in the early

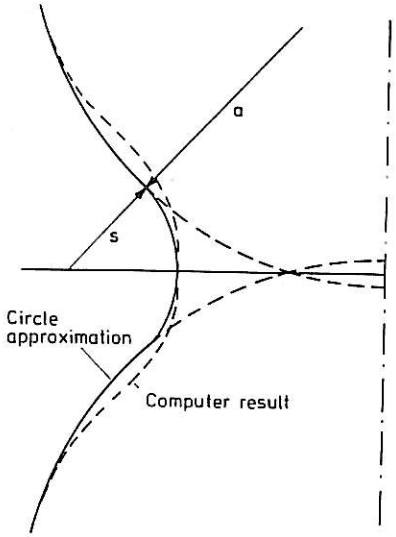

Fig. 7. Computer simulation of neck formation between two spherical particles for superimposed surface- and grain-boundary diffusion (a and s: compare fig. 5. $x/a = 0.58$). Note the agreement with experimental results shown in fig. 6. (From BROSS and EXNER [1979].)

stages of solid-state sintering are now well understood, and the general findings give a sound basis for a qualitative understanding of the later stages and more complex geometries as, for example, for contacts between pressed spheres (WELLNER *et al.* [1974]), spheres of different diameter (COBLE [1973]), for nonspherical geometries (USKOKOVIĆ and EXNER [1977]) and for models consisting of three or more particles (EXNER [1979a]).

Nearly unsurmountable problems are present when a concise quantitative description of the sintering behaviour of real powder compacts is attempted by extrapolating the results derived for two-particle models to multiparticle systems. Shrinkage equations have been derived in a straightforward way by simply assuming that the relative linear shrinkage, $\Delta L/L$, is equal to the ratio of centre-approach and particle diameter, h/a. Thus, the well-known and frequently applied power-law shrinkage relationship dating back to KINGERY and BERG [1955] is obtained:

$$\Delta L/L = h/a = ct^n, \tag{6}$$

where: $\Delta L/L$ = relative linear shrinkage, c, n = constants, t = sintering time. However, this extrapolation has no relevance and determination of the exponent n from shrinkage experiments with powder compacts (which was highly popular during the last three decades) is of no use for identifying the dominant sintering mechanism. To prove this fact, fig. 8 shows the pronounced difference of individual relative centre approach and shrinkage values measured for irregular planar arrays of copper

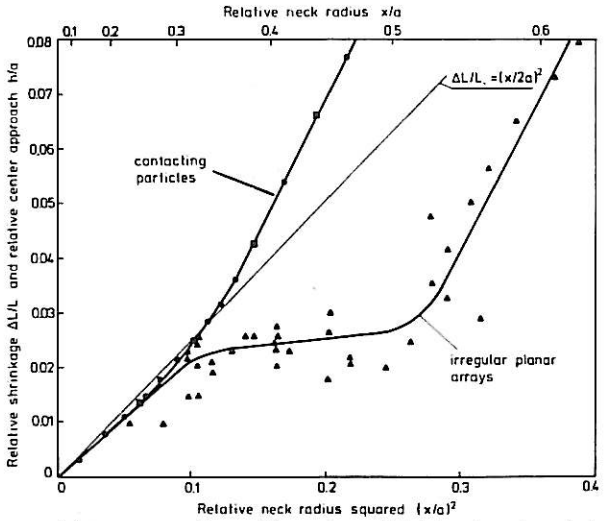

Fig. 8. Centre approach between contacting particles and overall shrinkage in an irregularly packed planar array of equally sized copper spheres sintered at 1300 K. The straight line corresponds to eq. (2). Note the pronouncedly lower shrinkage for the irregular array than predicted from centre approach. (From EXNER [1979a].)

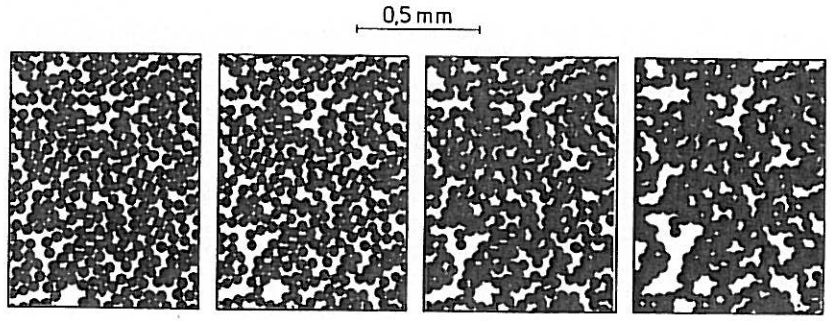

Fig. 9. Planar array of spherical copper particles sintered at 1300 K. Identical field at different stages (from left to right: presintered for 1 min, sintered for 2, 5 and 25 h). Note the local shrinkage and opening of large void regions. (From EXNER [1979a].)

spheres. The reason is that particles shift positions, contacts form or break up, and pores open up owing to rearrangement processes (fig. 9). Though uniform packing and pressing reduce these differences (EXNER *et al.* [1973] and EXNER [197a]), particle shapes typical for technical powders, local variations in packing, asymmetric contact geometry, and stresses induced by nonuniform particle size and packing may cause pronounced rearrangement and deviations from uniform shrinkage and thus invalidate eq. (6) for most practical applications. EVANS [1982] has shown that the stresses induced by inhomogeneous shrinkage may be large enough to open cracks as frequently observed in sintered ceramic compacts.

The decisive part of shrinkage takes place during a sintering stage where the individual necks and powder particles grow together and cannot be clearly identified any longer. The pore space then is still a continuous network embedded in an (obviously) continuous solid. During this stage, porosity is attached to the grain boundaries (or vice versa). Simple geometric, statistical and stereological models have proven useful for describing this situation (see EXNER [1980]). The most successful model, designed by COBLE [1961], has been a geometrically simple arrangement of cylindrical pores situated along the edges of regularly polyhedral grains. The flow of vacancies to each of these cylindrical pores is independent of its radius, r, because the higher curvature of a thin pore channel (proportional to $1/r$) is compensated by its smaller area for the arriving atoms (proportional to r). A cubic time-dependence for grain growth (increase of edge length of the polyhedral grains) and diffusional creep as rate-controlling mechanisms are assumed. This model yields a logarithmic dependence of porosity, P, upon sintering time t:

$$P_0 - P = k \ln t/t_0, \tag{7}$$

where P_0 and t_0 are porosity and time at the beginning of isothermal sintering, respectively. The cubic relationship for grain growth has repeatedly been confirmed for porous materials while, as pointed out in ch. 25, § 4.1, a quadratic relationship is

References: p. 1908.

typical for pure dense metals. The linear dependence of porosity on the logarithm of time has been found to fit many of the experimental results obtained with powders of alumina, copper, silver, iron, cobalt and nickel (for references see EXNER [1979a]). More recently, refined versions of this model have been published (e.g. BEERE [1975], KUCZYNSKI [1975, 1978], EADIE *et al.* [1978] and WONG and PASK [1979]). Its interesting aspects are the very clear connection between grain growth and densification and the extreme simplicity of the geometric and thermodynamic reasoning.

Table 3 shows a systematic survey of these and other popular concepts for deriving equations for isothermal shrinkage (linear or volume shrinkage, increase of density, or decrease of porosity) together with some major objections (EXNER [1980]). Each of these concepts has merits in focusing attention on particular aspects of the sintering process. The equations derived analytically or empirically were often applied to a variety of materials with little awareness of the critical assumptions implied. Nevertheless, excellent agreement with experimental data has been obtained. This is due to the fact that most equations contain more than one adjustable parameter, which makes it difficult to reach conclusive differentiation of the quality of different sintering equations (and the underlying ideas) on the basis of quality of fit (PEJOVNIK *et al.* [1979]).

Table 3
Basic concepts for deriving quantitative relationships for shrinkage kinetics of powder compacts (after EXNER [1980]).

Basic concept	Authors	Critical remarks
Extrapolation of idealized models:		
Two-particle model	KINGERY AND BERG [1955] COBLE [1958, 1970] ROCKLAND [1967]	Nonrealistic assumptions on neck shape. Effects of asymmetry and rearrangement not considered. Explicit equations valid only for single mechanism. Not applicable to later sintering stages.
Simple-pore model	COBLE [1961]	Geometry greatly oversimplified. Empirical grain-growth relationship.
Statistical approach	KUCZYNSKI [1978]	Simplifying geometric assumption on pore shape (no convex interfaces).
Rheological approach	SKOROKHOD [1972]	Defect geometry and interaction porosity–defects not clearly defined. Phenomenological definition of viscosity.
Sterological approaches	JOHNSON [1972] AIGELTINGER and DROLET [1974]	Integration of rate equation not possible. Phenomenological introduction of geometric parameters. Valid for early or late sintering stage, respectively.
Empirical approaches	TIKKANEN and MÄKIPIRTTI [1965]	Posterior motivation of empirical equation on basis of vacancy– dislocation interaction.
	IVENSEN [1973]	Posterior motivation of ad hoc equation based on non-defined defects. 3 adjustable parameters.
	Other authors (for references see EXNER [1979a])	Mathematical derivations or phenomenological and purely pragmatic equations without reasonable physical support.

In the very late stages of sintering (below 10% porosity), when isolated and geometrically well defined pores are present, a more realistic modelling of the behaviour of real materials is possible. Especially in ceramics, where high density values are striven for, breakaway of grain boundaries from the pores is the pre-eminent barrier to complete densification (see next section). In the light of the extensive efforts to give a proper theoretical basis to sintering processes, it is interesting to note that the techniques for improving sintering behaviour of materials which are difficult to densify have been developed essentially empirically. To date, the effects of dopants, such as transition metals in tungsten or MgO in Al_2O_3, which activate sintering dramatically, or the influence of the composition of sintering atmospheres, are still a matter of controversy (see, for example, GERMAN and MUNIR [1982]).

In addition, the effects of compacting, density distribution, contact geometry, structural defects, impurities and other factors of influence are understood for specific cases but not in terms of a general theory, and further work will be needed to close some of these gaps.

1.4. Development of microstructure and grain growth

The initial state of microstructure in a pressed compact is characterized by the microstructure of the individual particles and the shape of the pore space which, in turn, is determined by the shape and the arrangement of the particles. During the initial stage of sintering, grain boundaries develop at the contact regions, and the grain structure in the particles changes quickly by recrystallization if deformation during pressing has exceeded a critical value. The microstructure is then characterized by a continuous pore space with grain boundaries located at the small cross-sections of the solid. Further development of microstructural geometry (i.e. shape, dimensions and topological arrangement of porosity and grain-boundary network) can be assessed by quantitative microscopy (ch. 10A, § 2.4). Descriptive work using stereological and topological parameters (DE HOFF and AIGELTINGER [1970], AIGELTINGER and EXNER [1972], JERNOT *et al.* [1980] and CHERMANT *et al.* [1981]) shows that the geometric changes related to the reduction of pore volume are fairly similar for most materials. During the intermediate stage, the pore space forms a continuous network attached to grain boundaries, and the dimensions of the pore cross-section and the grains are related in much the same way as predicted by the

References: p. 1908.

Zener relationship (KUCZYNSKI [1975]):

$$R = k\frac{r}{P}, \tag{8}$$

where R and r are typical average dimensions of the grains and the porosity, respectively (e.g., mean linear intercepts or area-equivalent radii of planar cross-sections). The constant k is of the order of unity and related to the shape and to the size-distribution of the grains and the cross-sections of the pore network (see also ch. 25, § 3.7).

Only later in the sintering process, when the continuous pore system breaks down, are more or less equilibrium-shaped isolated pores formed at the grain boundaries (fig. 10). Theoretical studies show how the grain-growth kinetics are influenced by pores (MOCELLIN and KINGERY [1973], CARPAY [1977], CAHN [1980], HSUEH *et al.* [1982], SPEARS and EVANS [1982] and WEI and GERMAN [1982]). Pores can be dragged by grain boundaries and coalesce when meeting at grain edges or corners until they break away from the grain boundaries. The separation limits final densification since volume diffusion is usually much slower than grain-boundary diffusion. Additionally, local breakaway results in exaggerated grain growth or secondary recrystallization (ch. 25, § 4.3). Thus, the separation process is a decisive step in final-stage sintering, determining the microstructural details as well as the remaining porosity.

Grain-boundary motion, pore drag, pore shrinkage, pore coalesence, and pore detachment from grain corners, edges and facets have been modelled in order to explain the effects or process variables as heating rate, sintering time, sintering temperature, dopants etc. (COBLE and CANNON [1978], HSUEH *et al.* [1982] and SPEARS and EVANS [1982]). Figure 11 shows schematically the dependence of pore size on grain size and the conditions under which the pores become separated from the grain boundaries. Two pore-grain trajectories are indicated, one of which indicates a technically advantageous sintering route leading to full densification and

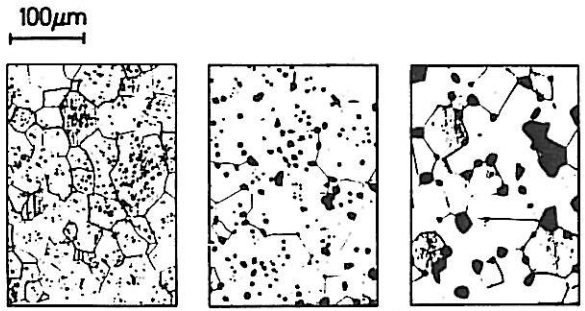

Fig. 10. Typical microstructures of sintered materials at late sintering stages. In carbonyl iron (left) the pores are mostly separated from grain boundaries, in magnesia (middle) small pores lie inside grains and the larger ones on grain boundaries, and in zinc oxide (right) most pores are on grain boundaries and corners. (From EXNER [1979b].)

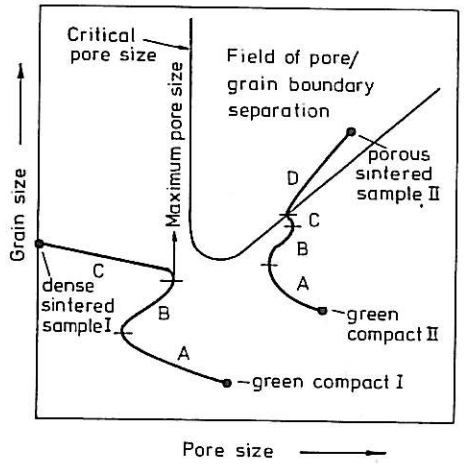

Fig. 11. Schematic plot of theoretical results indicating the relationship between pore and grain size in the final sintering stages. Sample I: favourable path for high final density. Sample II: path for porous product. A: rearrangement and densification by contact formation. B: intermediate stage shrinkage and coarsening. C: normal grain growth and final densification. D: pore–grain boundary separation, exaggerated grain growth, Ostwald ripening of isolated pores and cease of densification. (After SPEARS and EVANS [1982].)

a fine grain microstructure, while the second one enters the pore-detachment region resulting in residual porosity and coarse microstructure. In spite of the detailed models and derivations, equations describing these processes and their interactions, care must be taken not to carry the conclusions too far for practical cases. There are still many assumptions unproven by experimental facts (see, for example, CAHN [1980]). On the other hand, however, one should be able to optimize sintering conditions on this basis in order to obtain taylor-made microstructures in sintered materials, and to better understand the pronounced effects of special heating schedules such as rate-controlled heating (HUCKABEE *et al.* [1978]), quasi-isothermal heating (SOERENSEN [1980]), rapid sintering (BROOK [1969]), etc., by comparing the experimental findings with theoretical approaches and ideas.

2. *Hot pressing (pressure-sintering)*

Powders which are difficult to sinter can be consolidated to high density and strength by simultaneous application of heat and pressure. Such a process may be thought of as sintering enhanced by a pressure (*pressure-sintering*) or as a pressing operation activated by high temperatures (*hot-pressing*). The pressure allows lower temperatures than in pressureless sintering to be employed; thus normal grain

growth can be reduced and abnormal or exaggerated grain growth, caused by breakaway of grain boundaries from pores, may be avoided. If the pressure is applied uniaxially, the process is commonly referred to as hot-pressing, while *hot Isostatic pressing* (HIP, for short) utilizes hydrostatic pressure. The HIP process in particular has attained the position of the leading hot consolidation process; presses are commercially available which allow hydrostatic pressure, transmitted by gas, to be applied to a large heated volume (HANES *et al.* [1977] and FISCHMEISTER [1978]). Examples of its successful application are the production of tool steels, of superalloys, of alumina (e.g. for nuclear waste encapsulation), and of ceramic cutting tools.

2.1. Stresses and mechanisms

When an external pressure is applied to a hot powder compact, it is transmitted through the powder bed as a set of forces acting across the particle contacts. The exact force distribution depends on the stress state: in uniaxial hot-pressing some of the pressure is dissipated by die-wall friction, while HIP produces a uniform distribution resulting in more homogeneous densification. The local contact force per unit contact area (the "effective pressure") may exceed the capillary stress by several orders of magnitude, especially in the early stages of densification. This high stress not only enhances the diffusional processes contributing to pressureless sintering, but also introduces new densifying mechanisms. When the pressure is first applied, the contacts between the particles are small and the effective pressure will be sufficient to cause instantaneous plastic yielding in the contact zone. The resulting contact flattening leads to a rapid attenuation of the effective pressure until yielding stops. Then time-dependent deformation mechanisms determine the rate of further densification: power-law creep and stress-enhanced diffusion from a grain-boundary source to the neck surface, as in pressureless sintering. The contribution of vapour transport is even more insignificant than in pressureless sintering because it is not enhanced by the applied pressure.

It is convenient to divide the densification process into two stages (sometimes a third, intermediate stage is assumed which bridges the two mentioned here). During the initial stage the individual particles, which are commonly assumed to be spherical, can still be distinguished. The densification is determined by the deformation of the particle contacts caused by the local effective pressure acting on the contact area. In isostatic compaction, this effective pressure, σ, is proportional to the applied pressure, p (KAKAR and CHAKLADER [1968], COBLE [1970] and MOLERUS [1975]), e.g.:

$$\sigma = \frac{4\pi a^2}{AZ\rho} p, \tag{9}$$

where a is the particle radius, ρ the relative density of the compact (volume fraction of the solid), and A and Z are the average contact area and number of contacts per particle, respectively. Under certain assumptions concerning the structure of the particle-packing and the contact geometry, A and Z can be expressed as functions of ρ (ARZT [1982] and FISCHMEISTER and ARZT [1983]).

During the final stage, at relative densities greater than roughly 90%, the compact is usually modelled as a homogeneous solid containing isolated spherical pores. The effective pressure causing densification is then identical with the applied pressure, unless gas trapped in the pores causes a back-pressure which may prevent the compact from reaching full density.

2.2. Densification models

Numerous theoretical models have been developed for the mechanisms leading to densification in pressure-sintering. The initial densification upon application of the pressure is due to *plastic yielding*, provided the effective stress [eq. (9)] exceeds the stress necessary for plastic flow of two contacting spheres. This stress is higher than the yield stress in simple compression, because the material around the contact zone acts as a constraint for plastic deformation. The appropriate slip-line field is similar to that of a punch indenting a flat surface (or a hardness indentation) for which the yield criterion requires (HILL [1960]):

$$\sigma \approx 3\sigma_y, \tag{10}$$

where σ is the indentation stress and σ_y the yield stress, at temperature, of the powder material in compression. Yielding enlarges the contact areas and, as a consequence of the resulting densification, increases the number of contacts per particle. Once the effective pressure [eq. (9)] drops below the indentation stress [eq. (10)], yielding stops.

If the applied pressure is high, the compact may instantaneously reach densities above 90%. It has then entered the "final stage" by yielding alone and its behaviour is better modelled as the plastic collapse of a thick spherical shell (TORRE [1948] and HEWITT *et al.* [1973]), which requires:

$$p = \tfrac{2}{3}\sigma_y \ln(1-\rho). \tag{11}$$

Densification by *power-law creep* has been considered only recently, although it is often the dominant densifying mechanism (WILKINSON and ASHBY [1975], MATTHEWS [1980] and ARZT *et al.* [1983]). Exact solutions for this case are difficult to obtain; an approximation for the densification rate whose validity has been confirmed (SWINKELS *et al.* [1983]) is given by:

$$\frac{d\rho}{dt} = f(\rho, G)\frac{x}{a}\dot{\epsilon}_0\left(\frac{\sigma}{3\sigma_0}\right)^n, \tag{12}$$

where σ_0 and n are material properties, $\dot{\epsilon}_0$ is proportional to the volume diffusivity, x is the radius of the contact area and $f(\rho, G)$ is a function of the density and the geometry only.

As a model for final-stage densification, the creep of a thick spherical shell can be analyzed. This leads to the following equation for the densification rate:

$$\frac{d\rho}{dt} = f(\rho)\dot{\epsilon}_o\left(\frac{3}{2n}\frac{\sigma}{\sigma_0}\right)^n, \tag{13}$$

References: p. 1908.

where $f(\rho)$ is a complicated function of the relative density ρ.

A common feature of densification by plastic flow and power-law creep is their independence of the particle size. Further, both mechanisms are highly stress-sensitive, and for this reason the calculation of the effective stress is critical. Second-order effects, such as the increasing number of particle contacts, which at constant external pressure implies diminishing contact forces, can become important (ARZT [1982]). Also the question of whether the pores remain cusp-like or sintering necks are formed can be of relevance (SWINKELS *et al.* [1983]).

Diffusion, which is the most important densifying mechanism in pressureless sintering, contributes to pressure-sintering, too. It is enhanced by an applied pressure, because the additional energy $\sigma\Omega$ is gained on removing an atom with the volume Ω from a grain boundary acted on by a compressive traction σ (HERRING [1950], COBLE [1970]). The total chemical-potential difference between the grain boundary and the neck surface is

$$\Delta\mu = \sigma\Omega + \gamma\Omega\left(\frac{1}{r_1} + \frac{1}{r_2}\right). \tag{14}$$

Under normal pressure-sintering conditions, the second term (the capillary stress) is negligible and the driving force for densification is provided only by the external pressure. Hence pressure-sintering by diffusion, unlike pressureless sintering, is not sensitive to the exact shape and curvature of the sintering necks, and simplifying assumptions about the contact geometry will be less critical.

The rate of densification by diffusion is proportional to the number of atoms deposited, per second, on the surface of the sintering necks:

$$\frac{\mathrm{d}\rho}{\mathrm{d}t} = g(\rho, \mathrm{G})\frac{bD_\mathrm{b} + sD_\mathrm{v}}{kT\,a^3}\Delta\mu. \tag{15}$$

Here D_b and D_v are the boundary and volume diffusivities, b is the boundary thickness, k is Boltzmann's constant, T the absolute temperature, and s is the radius of curvature of the neck surface. $g(\rho, \mathrm{G})$ is a function of the relative density and the geometry. Here the particle radius a is a critical variable: fine powders densify much faster by diffusion than do coarse powders. Since a stress biases the chemical potential in a linear manner [eq. (14)], the rate of diffusional densification is directly proportional to the effective stress. A similar equation describes diffusional densification during the final stage.

There are several complicating features of diffusional densification. One is the limited efficiency of grain boundaries as vacancy sinks, which may result in a quadratic stress-dependence of the densification rate or a complete suppression of densification below a threshold stress (ARZT *et al.* [1982], see also § 1.2). Another is the influence of impurity segregation at grain boundaries on the boundary diffusivity (ch. 13, § 6.2). Further, the redistribution, by surface diffusion, of atoms arriving at the neck by grain-boundary diffusion can become the rate-limiting process. This has been recognized in pressureless sintering (§ 1.3). Because a pressure will not enhance this redistribution process, the effect should be even more pronounced in pressure-sintering.

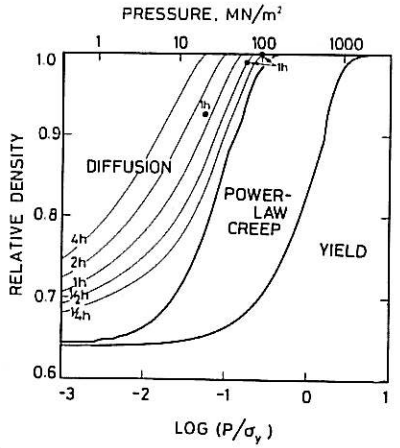

Fig. 12. A theoretical density–pressure diagram for hot-isostatic pressing (HIP) of a tool-steel powder with a particle radius of 25 μm, at a temperature of 1200°C. σ_y is the yield stress of the powder material. Data points correspond to typical industrial HIP cycles (with time marked in hours). Follow a vertical line (at a given external pressure p) in the direction of increasing density: the initial densification is due to plastic yielding of the particle contacts; at intermediate densities power-law creep in the contact zone dominates; diffusion may finally achieve full density. The thin lines are contours of constant time. (After ARZT *et al.* [1983].)

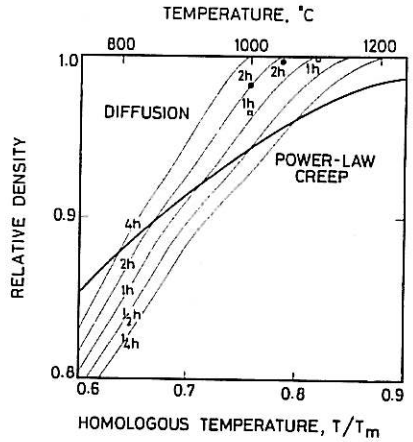

Fig. 13. The high-density portion of a density–temperature diagram for hot-isostatic pressing of the same powder as in fig. 12, at an applied pressure of 100 MN/m² (after ARZT *et al.* [1983]).

References: p. 1908.

2.3. Hot-pressing maps

This short treatment of the densifying mechanisms has established different dependences of the rate of densification on pressure, temperature, and particle size. For a given particle size, there are therefore distinct pressure–temperature regimes in which one mechanism is dominant, i.e. produces more densification than the others. This competition can be illustrated in theoretical diagrams (ARZT *et al.* [1983]), two of which are shown in figs. 12 and 13 for a tool-steel powder. The heavy lines bound the fields of dominance of one mechanism, while the superimposed thin lines are contours of constant time, which predict the extent of densification. It is seen, for example, that at a temperature of 1200°C and an applied pressure equal to a tenth of the yield stress of the powder material, power-law creep dominates up to a density of about 85%. Unless very high pressures are employed, the final densification is always due to diffusion. Therefore particle size is a critical variable. If the effective particle size is increased by grain growth, for instance, the dominance of power-law creep, which is insensitive to such a microstructural change, will be extended to higher densities.

Experimental data points typical of industrial HIP cycles are included in both figures; they are in promising agreement with the theoretical predictions. But it should be borne in mind that these and similar "maps" are based on a set of rate equations derived from simplifying assumptions as outlined above and depend on the knowledge of the appropriate material data which may vary considerably even within a specific grade of a technical alloy. At present, these maps are intended rather as a rational basis for designing HIP cycles, which in view of the high cost of HIP equipment is a worthwhile purpose. The maps also summarize conveniently our understanding of the pressure-sintering process: it is not one but several mechanisms which contribute to the densification. These mechanisms reflect the ways in which a stressed crystalline solid can deform. Pressure-sintering provides an example of a technical process in which the dominant deformation mechanism may change with time.

3. *Sintering with a liquid phase*

High-quality technical products can be made from mixed powders by cold compacting and then heating above the melting temperature of the lower-melting, low-volume-fraction (1–40 vol%) component. The shape of the compact is maintained as in solid state sintering, but higher densification levels are obtained as a rule.

Heavy metals (W with Cu, Fe, Ni), cemented carbides (WC, TiC with Co), ceramics containing glassy phases, aluminium, superalloys and cobalt–rare-earth magnets, and a variety of sintered steels are prominent examples (LENEL [1980]). The technical or economic reasons for applying this production process vary largely for these materials; reasons include the incapacity of other processes to produce

optimized microstructures with specified compositions and density, a need for reduced shaping cost, or a need for improved homogeneity. Usually, the original powder mixtures are not in chemical equilibrium at sintering temperature, at least in early stages, and chemical driving forces are present. Owing to the very low stresses needed for activating the flow of liquids, capillary forces play a major role even in non-equilibrium systems.

The shrinkage processes occurring during isothermal liquid state sintering are usually divided into three stages (HUPPMANN [1975] and LENEL [1980]):

(i) Rearrangement by liquid flow, retarded by friction between the solid particles. This stage requires good wetting since capillary forces acting at the liquid bridge are determined by the wetting angle (CAHN and HEADY [1970]).

(ii) Dense packing by shape-accommodation of particles separated by liquid films through solution and reprecipitation. This stage requires that the solid phase has a finite solubility in the liquid. In most systems this stage is connected with pronounced structural coarsening.

(iii) Skeleton formation and solid-state sintering. After the liquid is squeezed out between the particles, pores are removed by shrinkage of the solid skeleton. After full density is reached locally, interfacial and surface energy drive further shrinkage of the solid, and liquid is squeezed out into large void spaces (KWON and YOON [1980], KAYSSER *et al.* [1982]) or to the surface (RIEGGER *et al.* [1980]).

Neglecting all complicating factors (e.g. chemical driving forces, size and shape distribution of particles, bridging and coarsening effects), KINGERY [1959] has derived a quantitative description of shrinkage during isothermal liquid-phase sintering which results in equations of the type

$$\Delta V/V \approx 3\Delta L/L = kt^n, \tag{18}$$

where ΔV and V are the volume change and the initial volume, ΔL and L length change and initial length of the sample and k and n constants typical for each stage and mechanism involved. Application of this equation to compacts of metal and ceramic powder mixtures showed reasonable agreement, and conclusions on the rate-controlling steps were made on the basis of experimental values of n (e.g. 0.5 for reaction-controlled and 0.33 for diffusion-controlled solution/reprecipitation). In the light of later work (for references see HUPPMANN and PETZOW [1980] and LENEL [1980]) this agreement must be considered fortuitous or, by analogy with observations made with powders and solid-state sintering equations, due to a convenient fitting of two-parametric equations rather than to physical relevance.

In systems with appreciable solubility of the solid in the liquid phase (as in virtually all materials produced by liquid-phase sintering), the liquid penetrates particle bridges and grain boundaries in the early stages, which causes swelling if shrinkage by rearrangement is not rapid enough as, for example, in iron–copper alloys (BERNER *et al.* [1974], KAYSSER *et al.* [1980], TABESHFAR and CHADWICK [1982]). According to the classical second-stage mechanism (KINGERY [1959]), the capillary pressure at the contact points of the solid particles increases solubility and causes solution, transport through the liquid and reprecipitation at pressure-free

References: p. 1908.

solid–liquid interfaces. Additional and in most cases dominating driving forces for material transport through the liquid are caused by differences in surface curvature when irregular powders are concerned, and variations of defect densities or composition not only due to variations in the original powder particles but also due to the low defect density and the equilibrium composition of the reprecipitated parts (HUPPMANN and PETZOW [1980]). Though these effects do not directly affect the driving force for shrinkage exerted by porosity, they may contribute to densification and particle accommodation indirectly (HUPPMANN and PETZOW [1980] and LENEL [1980]). Finally, when a solid skeleton forms, shrinkage depends on solid state sintering mechanisms and follows the lines described in § 1.

Owing to the rapid material transport in liquids, coarsening of the microstructure is usually pronounced in liquid-phase sintering. Theories developed for coarsening (ripening) in dispersed systems (Wagner–Lifshits–Ardell theory for Ostwald ripening, see ch. 10B, § 3.2.2) apply to systems in which the amount of liquid is high (e.g., EXNER [1973]). In the typical range for liquid-phase sintering (volume fractions < 30%) or for systems with incomplete wetting of the solid by the liquid experienced with most combinations used in technical materials, the particles are in contact and coarsening will be effected by coalescence, i.e. grain-boundary movement assisted by reprecipitation of material into the energetically unfavourable grooves left behind. A concise theoretical treatment of liquid-phase densification and microstructural development is difficult owing to the complex interaction of mechanisms and processes involved. The basic phenomena are well understood, however, and a quantitative description of liquid-phase sintering for adequately realistic models seems feasible in the near future.

References

AIGELTINGER, E.H., and J.P. DROLET, 1974, in: Modern Developments in Powder Metallurgy, vol. 6, eds. H.H. Hausner and W.E. Smith (Metal Powder Industries Federation, Princeton, NJ) p. 323.

AIGELTINGER, E.H., and H.E. EXNER, 1972, J. Mater. Techn. 3, 425.

ALDINGER, F., 1974, Acta Metall. **22**, 923.

ALEXANDER, B.H., and R.W. BALLUFFI, 1957, Acta Metall. **5**, 666.

ARZT, E., 1982, Acta Metall. **30**, 1883.

ARZT, E., M.F. ASHBY and R.A. VERRALL, 1982, Technical Report CUED/C/MATS/TR60 (Cambridge University, Cambridge).

ARZT, E., M.F. ASHBY and K.E. EASTERLING, 1983, Metallurg. Trans. **14A**, 211.

ASHBY, M.F., 1969, Scripta Metall. **3**, 837.

ASHBY, M.F., 1972, Surf. Sci. **31**, 498.

ASHBY, M.F., 1974, Acta Metall. **22**, 275.

ASHBY, M.F., F. SPAEPEN and S. WILLIAMS, 1978, Acta Metall. **26**, 1647.

ASHBY, M.F., S. BAHK, J. BEVK and D. TURNBULL, 1980, Prog. Mater. Sci. **25**, 1.

BALSHIN, J.M., 1936, Vestn. Metalloprom. **16**, No. 17, 87.

BALLUFFI, R.W., 1980, Grain-Boundary Structure and Kinetics (ASM, Metals Park, OH).

BEERE, W., 1975, Acta Metall. **23**, 139.

BERNER, D., H.E. EXNER and G. PETZOW, 1974, in: Modern Developments in Powder Metallurgy, vol. 6, eds. H.H. Hausner and W.E. Smith (Metal Powder Industries Federation, Princeton, NJ) p. 237.

BRETT, J., and L.L. SEIGLE, 1963, Acta Metall. **11**, 467.

BROOK, R.J., 1969, J. Amer. Ceram. Soc. **52**, 56 and 339.

BROSS, P., and H.E. EXNER, 1979, Acta Metall. **27**, 1013.

CAHN, J.W., and R.B. HEADY, 1970, J. Amer. Ceram. Soc. **53**, 406.

CAHN, R.W., 1980, in: Recristallisation and Grain Growth of Multi-Phase and Particle Containing Materials, eds. N. Hansen, A.R. Jones and T. Leffers (Risø National Laboratory, Roskilde, Denmark) p. 77.

CARPAY, F.M.A., 1977, J. Amer. Ceram. Soc. **60**, 82.

CHERMANT, J.L., M. COSTER, J.P. JERNOT and J.L. DUPAIN, 1981, J. Microsc. **121**, 89.

CLARK, P.W., and J. WHITE, 1950, Trans. Brit. Ceram. Soc. **49**, 305.

COBLE, R.L., 1958, J. Amer. Ceram. Soc. **41**, 55.

COBLE, R.L., 1961, J. Appl. Phys. **32**, 787.

COBLE, R.L., 1970, J. Appl. Phys. **41**, 4798.

COBLE, R.L., 1973, J. Amer. Ceram. Soc. **56**, 461.

COBLE, R.L., and R.M. CANNON, 1978, in: Processing of Crystalline Solids, Materials Science Research, vol. 11, eds. H. Palmour, R.F. Davis and T.M. Hare (Plenum, New York) p. 151.

COBLENZ, W.S., J.M. DYNYS, R.M. CANNON and R.L. COBLE, 1980, in: Sintering Processes, Materials Science Research vol. 13, ed. G.C. Kuczynski (Plenum, New York) p. 141.

DEHOFF, R.T., and H.E. AIGELTINGER, 1970, in: Advanced Techniques in Powder Metallurgy, Perspectives in Powder Metallurgy, vol. 5, eds. J.S. Hirschhorn and K.H. Roll (Plenum, New York) p. 81.

EADIE, R.L., G.C. WEATHERLY and K.T. AUST, 1978, Acta Metall. **26**, 759.

EVANS, A.G., 1982, J. Amer. Ceram. Soc. **65**, 497.

EXNER, H.E., 1973, Z. Metallk. **64**, 273.

EXNER, H.E., 1979a, Rev. Powder Metallurg. Phys. Ceram. **1**, 7.

EXNER, H.E., 1979b, J. Microsc. **116**, 25.

EXNER, H.E., 1980, Powder Metallurg. **23**, 203.

EXNER, H.E., 1982, Met. Sci. **16**, 451.

EXNER, H.E., G. PETZOW and P. WELLNER, 1973, in: Sintering and Related Phenomena, Materials Science Research, vol. 6, ed. G.C. Kuczynski (Plenum, New York) p. 351.

FISCHMEISTER, H.F., 1978, Powder Metallurg. Int. **10**, 119.

FISCHMEISTER, H.F., and E. ARZT, 1983, Powder Metallurg., in press.

FISCHMEISTER, H.F., and H.E. EXNER, 1964, Metall **18**, 932;
1965, Metall **19**, 113.

FRENKEL, J., 1945, J. Phys. USSR **9**, 385.

GEGUZIN, J.A., 1973, Physik des Sinterns (VEB Deutscher Verlag für Grundstoffindustrie, Leipzig).

GERMAN, R.M., 1982, Sci. Sint. **14**, 13.

GERMAN, R.M., and Z.A. MUNIR, 1975, Metallurg. Trans. **6A**, 2223.

GERMAN, R.M., and Z.A. MUNIR, 1982, Rev. Powder Metallurg. Phys. Ceram. **2**, 9.

GESSINGER, G.H., 1970, Scripta Metall. **4**, 673.

GLEITER, H., 1969, Acta Metall. **17**, 565.

GLEITER, H., 1979, Acta Metall. **27**, 187.

HANES, H.D., D.A. SEIFFERT and C.R. WATTS, 1977, Hot Isostatic Processing (Metals and Ceramics Information Center, Columbus, OH).

HEDVALL, J.A., and E. HELIN, 1927, Jernkont. Ann. **82**, 265.

HERRING, C., 1950, J. Appl. Phys. **21**, 437.

HEWITT, R.L., W. WALLACE and M.C. DE MALHERBE, 1973, Powder Metallurg. **16**, 88.

HILL, R., 1960, The Mathematical Theory of Plasticity (Clarendon Press, Oxford) p. 254.

HOGE, C.E., and J.A. PASK, 1977, Ceramurgia Int. **3**, 95.

HSUEH, C.H., A.G. EVANS and R.L. COBLE, 1982, Acta Metall. **30**, 1281.

HUCKABEE, M.L., T.M. HARE and H. PALMOUR, 1978, in: Processing of Crystalline Solids, Materials Science Research, vol. 11, eds. H. Palmour, R.F. Davis and T.M. Hare (Plenum, New York) p. 205.

HÜTTIG, G.F., 1948, Arch. Metallk. **2**, 93.

HUPPMANN, W., 1975, in: Sintering and Catalysis, Materials Science Research, vol. 10, ed. G.C. Kuczynski (Plenum, New York) p. 359.
HUPPMANN, W., and G. PETZOW, 1980, in: Sintering Processes, Materials Science Research, vol. 13, ed. G.C. Kuczynski (Plenum, New York) p. 189.
ICHINOSE, H., and G.C. KUCZYNSKI, 1962, Acta Metall. **10**, 205.
IVENSEN, V.A., 1973, Densification of Metal Powders during Sintering (Consultants Bureau, New York, London).
JAEGER, W., and H. GLEITER, 1978, Scripta Metall. **12**, 675.
JERNOT, J.P., J.L. CHERMANT, P. MAIRE and P. GILES, 1980, Mikroskopie **37** (Suppl.), 331.
JOHNSON, D.L., 1970, Scripta Metall. **4**, 677.
JOHNSON, D.L., 1972, in: Powder Metallurgy for High Performance Applications, eds. J.J. Burke and V. Weiss (Syracuse Univ. Press) p. 139.
JONES, W.D., 1946, Metal Treatment **13**, 265.
KAKAR, A.K. and A.C.D. CHAKLADER, 1968, Trans. AIME **242**, 1117.
KAYSSER, W.A., W.J. HUPPMANN and G. PETZOW, 1980, Powder Metallurg. **23**, 86.
KAYSSER, W.A., O.J. KWON and G. PETZOW, 1982, in: P/M-82 in Europe, Preprints Intern. Powder Metallurgy Conference (Assoc. Italiana di Metallurgia, Milano) p. 23.
KING, A.H., and D.A. SMITH, 1980, Phil. Mag. **42**, 495.
KINGERY, W.D., and M. BERG 1955, J. Appl. Phys. **26**, 1205.
KINGERY, W.J., 1959, J. Appl. Phys. **30**, 301.
KUCZYNSKI, G.C., 1949, Metallurg. Trans. AIME **185**, 169.
KUCZYNSKI, G.C., 1975, in: Sintering and Catalysis, Materials Science Research, vol. 10, ed. G.C. Kuczynski (Plenum, New York) p. 325.
KUCZYNSKI, G.C., 1978, Science of Sintering, Monograph 17 (The Serbian Academy of Science and Arts, Beograd).
KUCZYNSKI, G.C., G. MATSUMURA and B.B. CULLITY, 1960, Acta Metall. **8**, 205.
KWON, O.J., and D.N. YOON, 1980, in: Sintering Processes, Materials Science Research, vol. 13, ed. G.C. Kuczynski (Plenum, New York) p. 203.
LENEL, F.V., 1980, Powder Metallurgy – Principles and Applications (Metal Powder Industries Federation, Princeton, NJ).
MACKENZIE, J.K., and R. SHUTTLEWORTH, 1949, Proc. Phys. Soc. **62**, 833.
MATTHEWS, J.R., 1980, Acta Metall. **28**, 311.
MISHRA, A., F.V. LENEL and G.S. ANSELL, 1975, in: Sintering and Catalysis, ed. G.C. Kuczynski (Plenum, New York) p. 339.
MOCELLIN, A., and W.D. KINGERY, 1973, J. Amer. Ceram. Soc. **56**, 309.
MOLERUS, O., 1975, Powder Techn. **12**, 259.
NABBARRO, F.R.N., 1967, Phil. Mag. **16**, 231.
NICHOLS, F.A., 1980, Scripta Metall. **14**, 951.
NICHOLS, F.A., and W.W. MULLINS, 1965, J. Appl. Phys. **36**, 1826.
NILSSON, J.-O., P.R. HOWELL and G.L. DUNLOP, 1979, Acta Metall. **27**, 179.
NUNES, J.J., F.V. LENEL and G.S. ANSELL, 1971, Acta Metall. **19**, 107.
PEJOVNIK, S., V. SMOLEJ, D. SUSNIK, and D. KOLAR, 1979, Powder Metallurg. Int. **11**, 22.
PINES, B.J., 1946, Zh. Tekh. Fiz. **16**, 737.
RIEGGER, H., J.A. PASK and H.E. EXNER, 1980, in: Sintering Processes, Materials Science Research, vol. 13, ed. G.C. Kuczynski (Plenum, New York) p. 219.
ROCKLAND, J.G.R., 1967, Z. Metallk. **58**, 467 and 564.
ROSS, J.W., W.A. MILLNER and G.S. WEATHERLY, 1982, Z. Metallk. **73**, 391.
ROTH, T.A., 1975, Mater. Sci. Eng. **18**, 183.
SCHATT, W., ed., 1981, Einführung in die Werkstoffwissenschaft (VEB Deutscher Verlag für Grundstoffindustrie, Leipzig).
SCHATT, W., H.E. EXNER, E. FRIEDRICH and G. PETZOW, 1982, Acta Metall. **30**, 1367.
SCHOBER, T., and R.W. BALLUFFI, 1970, Phil. Mag. **21**, 109.

SHALER, A.J., and J. WULFF, 1948, Ind. Eng. Chem. **40**, 838.
SKOROKHOD, V.V., 1972, Rheologicheskie Osnovy Teorii Spekania (Rheological Theory of Sintering) (Izd. Naukovaya Dumka, Kiew).
SOERENSEN, O.T., 1980, in: Thermal Analysis (Birkhäuser, Basel) p. 231.
SPEARS, M.A. and A.G. EVANS, 1982, Acta Metall. **30**, 1281.
SWINKELS, F.B., and M.F. ASHBY, 1980, Powder Metallurg. **23**, 1.
SWINKELS, F.B., and M.F. ASHBY, 1981, Acta Metall. **29**, 259.
SWINKELS, F.B., D.S. WILKINSON, E. ARZT and M.F. ASHBY, 1983, to be published.
TABESHFAR, K., and G.A. CHADWICK, 1982, in: P/M-82 in Europe, Preprints Intern. Powder Metallurgy Conference (Assoc. Italiana di Metallurgia, Milano) p. 693.
TAMMANN, G., 1926, Z. Anorg. Allg. Chem. **157**, 321.
THÜMMLER, F., and W. THOMMA, 1966, in: Modern Developments in Powder Metallurgy, vol. 12, ed. H.H. Hausner (Plenum, New York) p. 3.
THÜMMLER, F., and W. THOMMA, 1967, Metallurg. Rev. **12**, 69.
TIKKANEN, M.H., and S.A. MÄKIPIRTTI, 1965, Int. J. Powder Metallurg. **1**, No. 1, 15.
TORRE, C., 1948, Berg- u. Hüttenm. Mh. **93**, 62.
UDIN, H., A.J. SHALER and J. WULFF, 1949, Metallurg. Trans. AIME **185**, 186.
USKOKOVIC, D., and H.E. EXNER, 1977, Phys. Sint. **9**, 265.
WEI, T.S., and R.M. GERMAN, 1982, in: P/M-82 in Europe, Preprints Intern. Powder Metallurgy Conference (Assoc. Italiana di Metallurgia, Milano) p. 239.
WELLNER, P., G.H. GESSINGER and H.E. EXNER, 1974, Z. Metallk. **65**, 602.
WILKINSON, D.S., and M.F. ASHBY, 1975, Acta Metall. **23**, 1277.
WONG, B., and J.A. PASK, 1979, J. Amer. Ceram. Soc. **62**, 138.

Further Reading

Burke, J.J., and V. Weiss, eds., 1972, Powder Metallurgy for High-Performance Application (Syracuse University Press, Syracuse).
Exner, H.E., 1978, Grundlagen von Sintervorgängen (Gebr. Borntraeger Verlag, Stuttgart), in German, English translation by V.F. Lenel published 1980, Rev. Powder Metallurg. Phys. Ceram **1**, 7.
Geguzin, J.E., 1973, Physik des Sinterns (VEB Deutscher Verlag für Grundstoffindustrie, Leipzig).
Hanes, H.D., D.A. Seiffert and C.R. Watts, 1977, Hot Isostatic Processing (Metals and Ceramics Information Center, Columbus, Ohio).
Lenel, V.F. 1980, Powder Metallurgy – Principles and Applications (Metal Powder Industries Federation, Princeton, NJ).
Schatt, W., ed., 1977, Pulvermetallurgie, Sinter- und Verbundwerkstoffe (VEB Deutscher Verlag für Grundstoffindustrie, Leipzig).
Thümmler, F., and W. Thomma, 1967, Metallurg. Rev. **12**, 69.

The following journals and book series are specialized in powder metallurgy and topics treated in this chapter are frequently discussed:

Journals

Science of Sintering (edited by the International Institute for the Science of Sintering, Beograd, Yugoslavia).
Powder Metallurgy International (edited by Schmid-Verlag, Freiburg, FR-Germany).
Powder Metallurgy (edited by The Metals Society, London, UK).
International Journal of Powder Metallurgy (edited by Metal Powder Industries Federation, Princeton, NJ, USA).
Soviet Powder Metallurgy and Metal Ceramics (translated from Russian by Consultants Bureau, New York, USA).

Reviews in Powder Metallurgy and Physical Ceramics (edited by G. Freund Publishing House, Tel Aviv, Israel).
Planseeberichte für Pulvermetallurgie (Metallwerk Plansee AG, Reutte) discontinued 1981.

Book series

Materials Science Research (Plenum Press, New York, London):
Vol. 6, 1973, G.C. Kuczynski, ed., Sintering and Related Phenomena.
Vol. 9, 1975, A.R. Cooper and A.H. Heuer, eds., Mass Transport Phenomena in Ceramics.
Vol. 10, 1978, G.C. Kuczynski, ed., Sintering and Catalysis.
Vol. 13, 1980, G.C. Kuczynski, ed., Sintering Processes.
Vol. 14, 1981, J. Pask and A. Evans, eds., Surfaces and Interfaces in Ceramic and Ceramic Metal Systems.
Modern Developments in Powder Metallurgy, Proceedings of the International Powder Metallurgy Conferences (Metal Power Industries Federation, Princeton, NJ, USA).
Perspectives in Powder Metallurgy – Fundamentals, Methods and Applications (Plenum, New York, London).
New Perspectives in Powder Metallurgy (Metal Powder Industries Federation, Princeton, NJ, USA).
Progress in Powder Metallurgy, Proceedings of the National US Powder Metallurgy Conferences (Metal Powder Industries Federation, Princeton, NJ, USA).

AUTHOR INDEX